*Stanford Exploration Project, Report 123, October 31, 2005, pages 83–??*

# Short Note

# Target-oriented wave-equation inversion: Sigsbee model

*Alejandro A. Valenciano, Biondo Biondi, and Antoine Guitton*[1]

## INTRODUCTION

Sigsbee model is often used as a benchmark for migration/inversion algorithms due to its geological complexity. The data was modeled by simulating the geological setting found on the Sigsbee escarpment in the deep-water Gulf of Mexico. The model exhibits illumination problems due to the complex salt shape, with a rugose salt top.

When the subsurface is complex, migration operators produce images with reflectors correctly positioned but biased amplitudes (Prucha et al., 2000; Kuehl and Sacchi, 2001). That is why an inversion formalism (Tarantola, 1987) needs to be used to account for that problem.

In this paper, we apply the target-oriented wave-equation inversion idea presented in Valenciano et al. (2005) to the Sigsbee data. Due to the complex velocity structure and the limited acquisition cable length, the reflectors are not illuminated from all reflection angles. That highlights the need of a more sophisticated regularization in the angle domain (Prucha et al., 2000; Kuehl and Sacchi, 2001; Valenciano and Biondi, 2005) than the simple damping proposed by Valenciano et al. (2005).

## INVERSION SETTING

### Linear least-squares inversion

Tarantola (1987) formalizes the geophysical inverse problem by giving a theoretical approach to compensate for experiment deficiencies (e.g., acquisition geometry, obstacles), while being consistent with the acquired data. His approach can be summarized as follows: given a linear modeling operator $\mathbf{L}$ compute synthetic data, $\mathbf{d}$, using,

$$\mathbf{d} = \mathbf{L}\mathbf{m}, \tag{1}$$

where $\mathbf{m}$ is a reflectivity model, and given the recorded data $\mathbf{d}_{obs}$, a quadratic cost function,

$$S(\mathbf{m}) = \|\mathbf{d} - \mathbf{d}_{obs}\|^2 = \|\mathbf{L}\mathbf{m} - \mathbf{d}_{obs}\|^2, \tag{2}$$

[1]**email:** valencia@sep.stanford.edu, biondo@sep.stanford.edu, antoine@sep.stanford.edu

is formed. The model of the earth $\hat{\mathbf{m}}$ that minimizes $S(\mathbf{m})$ is given by

$$\hat{\mathbf{m}} = (\mathbf{L}'\mathbf{L})^{-1}\mathbf{L}'\mathbf{d}_{obs} \quad (3)$$

$$\hat{\mathbf{m}} = \mathbf{H}^{-1}\mathbf{m}_{mig}, \quad (4)$$

where $\mathbf{L}'$ (migration operator) is the adjoint of the linear modeling operator $\mathbf{L}$, $\mathbf{m}_{mig}$ is the migration image, and $\mathbf{H} = \mathbf{L}'\mathbf{L}$ is the Hessian of $S(\mathbf{m})$.

The main difficulty with this approach is the explicit calculation of the Hessian inverse. In practice, it is more feasible to compute the least-squares inverse image as the solution of the linear system of equations

$$\mathbf{H}\hat{\mathbf{m}} = \mathbf{m}_{mig}, \quad (5)$$

by using an iterative conjugate gradient algorithm.

Another difficulty with this approach is that the explicit calculation of the Hessian for the entire model space is impractical. Valenciano and Biondi (2004) and Valenciano et al. (2005) discuss a way to make this problem more tractable.

### Non-stationary least-squares filtering

The condition number of the target-oriented Hessian matrix can be high, making the solution of the non-stationary least-squares filtering problem in equation (5) unstable. One solution is adding a smoothing regularization operator to equation (5):

$$\begin{aligned} \mathbf{H}\hat{\mathbf{m}} - \mathbf{m}_{mig} &\approx 0, \\ \epsilon\mathbf{I}\hat{\mathbf{m}} &\approx 0, \end{aligned} \quad (6)$$

where the choice of the identity operator ($\mathbf{I}$) as regularization operator is customary. A more sophisticated regularization scheme could involve applying a smoothing operator in the reflection angle (or offset ray-parameter) dimension (Prucha et al., 2000; Kuehl and Sacchi, 2001) or, more generally, in the reflection and azimuth angles as proposed by Valenciano and Biondi (2005).

## NUMERICAL RESULTS: SIGSBEE MODEL

The Sigsbee data set was modeled by simulating the geological setting found on the Sigsbee escarpment in the deep-water Gulf of Mexico. The model exhibits the illumination problems due to the complex salt shape, characterized by a rugose salt top (see Figure 1). We choose a target zone (indicated with the "target" box in Figure 1) to see the effects of illumination on imaging close to the salt.

Figure 2 shows the shot-profile migration image (using cross-correlation imaging condition) corresponding to the portion of Sigsbee model shown in figure 1. Notice how the

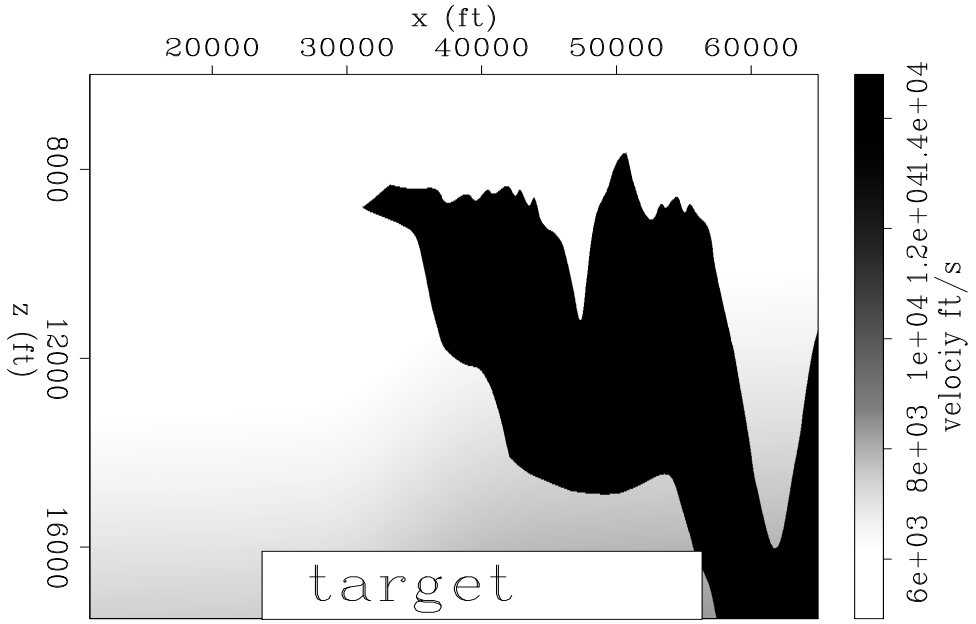


Figure 1: Sigsbee velocity model, target zone indicated with the "target" box. alejandro2-Sis_vel [CR]

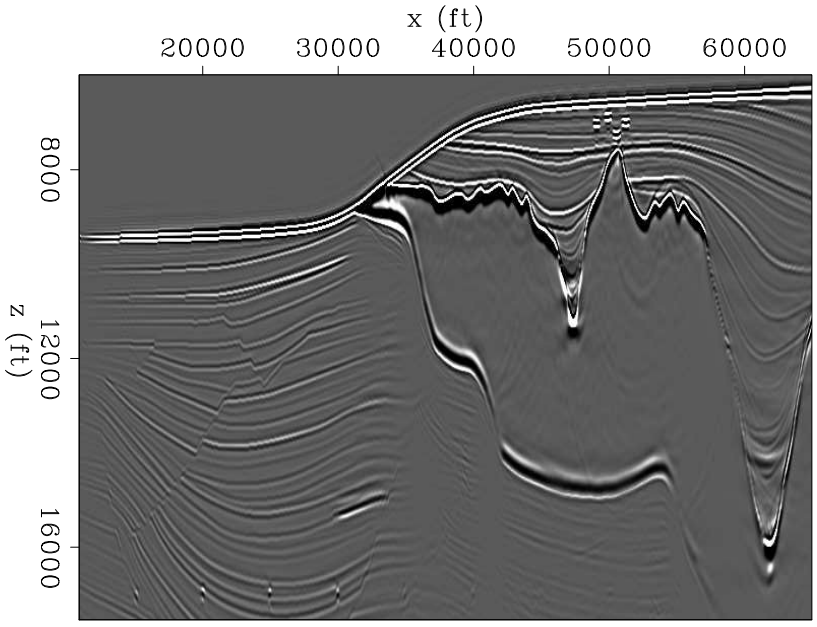


Figure 2: Sigsbee shot-profile migration image using cross-correlation imaging condition. alejandro2-mig_Sis [CR]

diffractor amplitudes located at 17000 feet depth fade away as they get closer to the salt. The same happens to the reflectors as they get close to the salt.

Figure 3 shows a $21 \times 7$ coefficient filter (target-oriented Hessian) at constant depth as the $x$ coordinate moves from the sediments to the salt boundary. Figure 3a shows point 1, with coordinates $\mathbf{x} = (17000, 30000)\ ft$ (far from the salt). Figure 3b shows point 2, with coordinates $\mathbf{x} = (17000, 34000)\ ft$. Figure 3c shows point 3, with coordinates $\mathbf{x} = (17000, 38000)\ ft$. Figure 3d shows point 4, with coordinates $\mathbf{x} = (17000, 42000)\ ft$ .

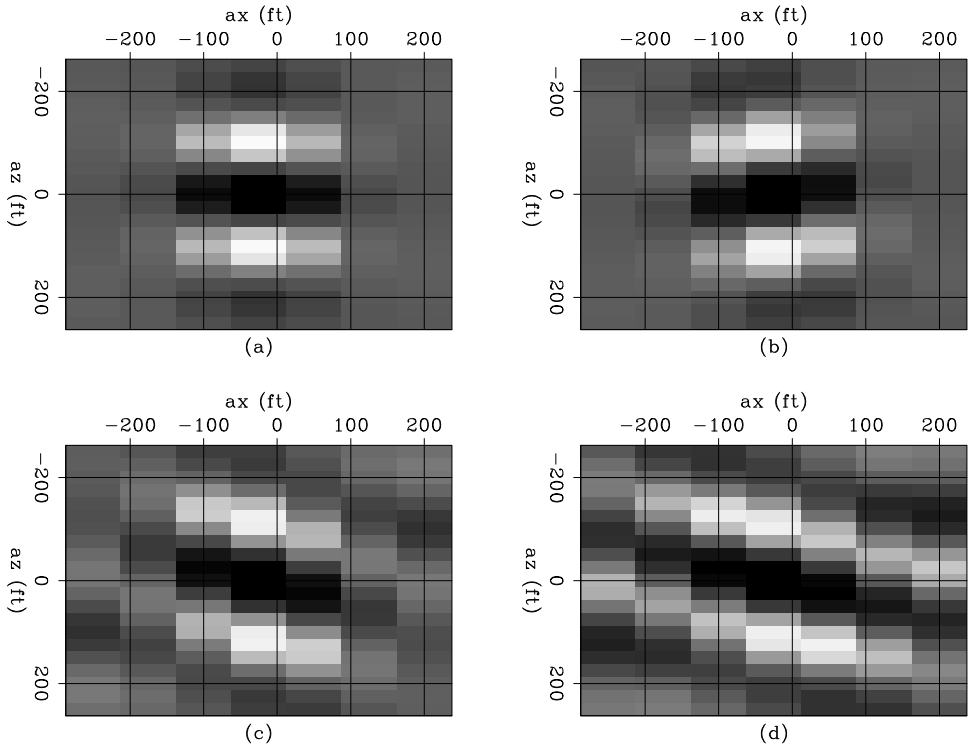


Figure 3: Hessian of the Sigsbee model, (a) point 1 $\mathbf{x} = (17000, 30000)\ ft$, (b) point 2 $\mathbf{x} = (17000, 34000)\ ft$, (c) point 3 $\mathbf{x} = (17000, 38000)\ ft$, and (d) point 4 $\mathbf{x} = (17000, 42000)\ ft$. alejandro2-hesian_phase_Sis [CR]

Unlike the constant velocity case (Valenciano et al., 2005), the shape of the filter is not dependent only on the acquisition geometry but the subsurface geometry (presence of the salt body). In the area unaffected by the salt the filter looks the same as is the constant velocity case, but as we get closer to the salt the illumination varies (in intensity and angle) and the filter behaves differently. This is due to a focusing and defocusing effect created by the salt. To correct this effect we computed the least-squares inverse image, by the method described in Valenciano et al. (2005).

Figure 4 shows a comparison between the migration and the inversion images in the target area. The stratigraphic model is shown in Figure 4a. Notice the seven equal-strength point diffractors and the position of the faults. Figure 4b shows the illumination, which is the diagonal of the Hessian matrix (dark is high illumination light is low illumination). Notice the decrease in the illumination as it gets closer to the salt with the exception of a narrow strip

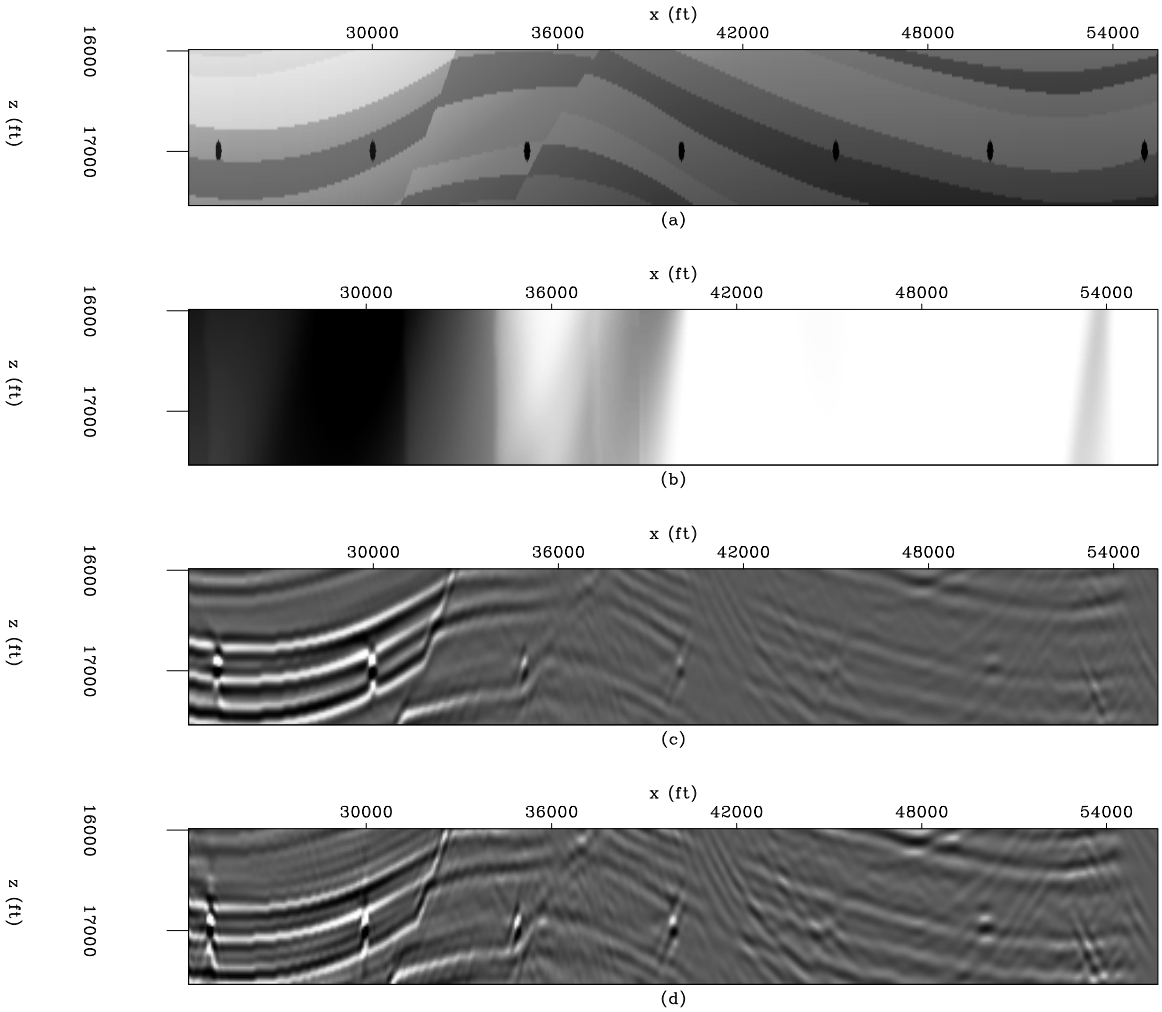


Figure 4: Target area comparison. (a) stratigraphic model, (b) illumination (dark is high and light is low), (c) migration, and (d) inversion. alejandro2-comp_Sis_full [CR]

where energy focuses close to the salt. The migration result is shown in Figure 4c. The reflectors dim out as they get closer to the salt. In contrast, Figure 4d shows the inversion result, the resolution increases (especially to the left of the image) and the section looks more balance. Also notice how the diffractors amplitude is better balanced.

At the right of the image the resolution did not increase as much as to the left. This is due to the fact that data values (migration) to the left are bigger than to the right (Figure 4c), and so are the data residuals. Thus, the solver expends most of the time decreasing the residuals in that area.

To test the previous hypothesis we did the inversion only in the low-illumination, reduced target area (Figure 5). Figure 5a shows the illumination (diagonal of the Hessian matrix) in the low-illumination area. Figure 5b shows the migration in the low-illumination area. Figure 5c shows the inversion performed in the full target area to match the dimensions of the inversion

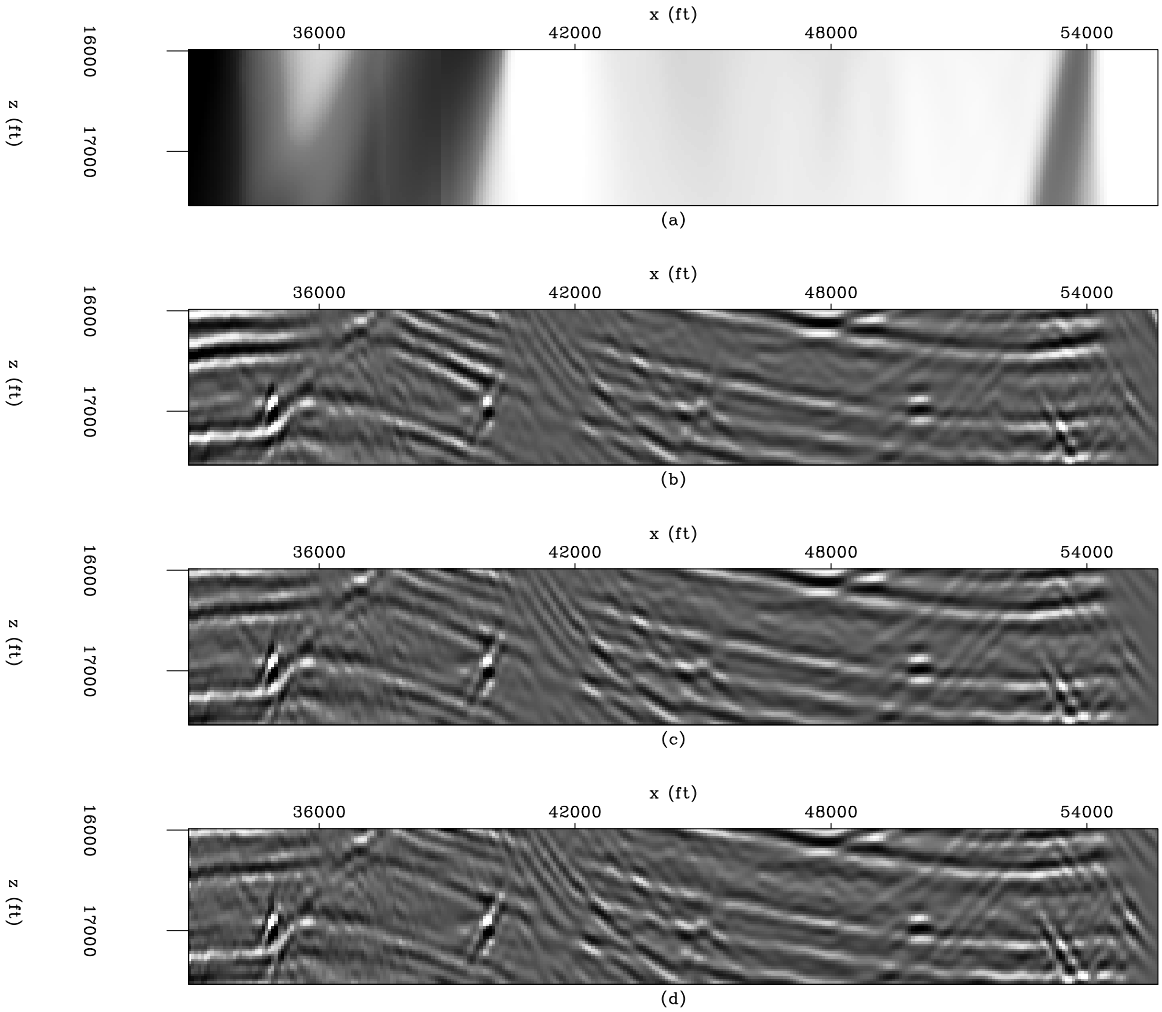


Figure 5: Reduced target area comparison. (a) illumination (dark is high and light is low), (b) migration, (c) inversion in the full target area, and (d) inversion in the reduced target area. alejandro2-comp_Sis_wind [CR]

on the low-illumination area which is shown in Figure 5d. There are substantial differences between the two inversion results: the result in the low-illumination area has better resolution than the one in the full target area, and the last diffractor (right corner) is more energetic in the result in the low-illumination than the one done in the full target area.

In general, even though inversion gives more balanced and better resolved images, it also produces more noisy results. Thus, a more sophisticated regularization might be necessary. Prucha et al. (2000) and Kuehl and Sacchi (2001) propose using a smoothing operator in the reflection angle (offset ray parameter) dimension. Valenciano and Biondi (2005) proposes a more general regularization in the reflection and azimuth angle dimensions.

## CONCLUSIONS

Imaging the Sigsbee model highlights the need of a regularization in the angle domain of the target-oriented wave equation inversion problem (Prucha et al., 2000; Kuehl and Sacchi, 2001; Valenciano and Biondi, 2005). Even though the inversion gives a more balanced sections and higher resolution images, it also increases the noise.

## REFERENCES

Kuehl, H., and Sacchi, M., 2001, Generalized least-squares DSR migration using a common angle imaging condtion: Soc. of Expl. Geophys., 71st Ann. Internat. Mtg, 1025–1028.

Prucha, M. L., Clapp, R. G., and Biondi, B., 2000, Seismic image regularization in the reflection angle domain: SEP–**103**, 109–119.

Tarantola, A., 1987, Inverse problem theory: Elsevier.

Valenciano, A. A., and Biondi, B., 2004, Target-oriented computation of the wave-equation imaging Hessian: SEP–**117**, 63–76.

Valenciano, A. A., and Biondi, B., 2005, Wave-equation angle-domain hessian: SEP–**123**.

Valenciano, A. A., Biondi, B., and Guitton, A., 2005, Target-oriented wave-equation inversion: SEP–**120**, 23–40.